arXiv:1210.6539v1 [cs.NE] 24 Oct 2012

Towards Swarm Calculus: Urn Models of Collective Decisions and Universal Properties of Swarm Performance

Heiko Hamann
Artificial Life Laboratory
of the Department of Zoology
Karl-Franzens University Graz,
Universitätsplatz 2,
A-8010 Graz, Austria,
heiko.hamann@uni-graz.at

October 25, 2012

Abstract

The search for generally applicable methods in swarm intelligence aims to gain new insights about natural swarms and to develop design methodologies for artificial swarms. The ideal would be a 'swarm calculus' that allows to calculate key features such as expected swarm performance and robustness on the basis of a few parameters. A path towards this ideal is to find methods and models that have maximal generality. We report two models that might be examples of exceptional generality. First, we present an abstract model that describes the performance of a swarm depending on the swarm density based on the dichotomy between cooperation and interference. Several examples are given how the model fits to results from typical swarm experiments. Second, we give an abstract model of collective decision making that is inspired by urn models. A parameter, that controls the feedback based on the current consensus, allows to understand the effects of an increasing probability for positive feedback over time in a decision making system. Several applicable methods, such as the description as Markov process, calculation of splitting probabilities, mean first passage times, and measurements of positive feedback, are discussed and applications to artificial and natural swarms are reported.

1 Introduction

Research in the context of swarm intelligence is important in biology to gain new insights about natural swarms and also in fields aiming for artificial swarms, such as swarm robotics, to obtain sophisticated design methodologies. Ideal tools would allow to calculate fundamental features of swarm behavior, such as performance, stability, and robustness, based on an input of a few observed parameters in the case of natural swarm systems or a few designed parameters in the case of artificial swarms. We call this highly desired set of tools 'swarm calculus' (calculus in its general sense). The idea is to establish a set of mathematical tools that can easily be applied to a variety of settings in the field of swarm intelligence and that can be combined in many ways by using them as mathematical building blocks for modeling. Thus, models will surely be an important part of swarm calculus.

In order to define a general methodology of understanding and designing swarm systems, general properties and generally applicable models need to be found. Today only few models exist that have the potential to become general swarm models. Biological swarm models are particularly distinguished by their variety (Okubo and Levin, 2001; Okubo, 1986; Vicsek and Zafeiris, 2012; Edelstein-Keshet, 2006; Camazine et al., 2001). Typically each biological challenge is answered by a specialized model. The desire for a model with applicability to all natural swarms seems to be small in that community. In the field of artificial swarms, such as robot swarms, the desire for generality seems to be bigger which is, for example, expressed by several models in swarm robotics (Hamann, 2010; Berman et al., 2011; Prorok et al., 2011; Milutinovic and Lima, 2007; Lerman et al., 2005). The idea of these models is to support the design of swarm robotic systems within a maximal range of applications. They focus on features that describe quantities of the swarm behavior, such as robot distributions or required times for certain tasks and typically struggle between the intended generality and having direct connections between the model and the actual description of the individual robot's behavior. If we abandon, however, the demand for a detailed description of behavioral features and focus only on high-level features such as overall performance or the macroscopic process of a collective decision then a higher degree of generality is achievable. In addition, that way it is possible to define concise mathematical descriptions that, in turn, allow applications of standard methods from statistics, linear algebra, statistical mechanics etc. In this paper, we identify two models of universal properties of swarm systems concerning the dependence of swarm performance on swarm density and the dependence of collective decisions on positive feedback. Next we give an introduction to each of the two fields.

1.1 Swarm performance

By 'swarm performance' we denote the efficiency of a swarm in a certain task. For example, the swarm performance can be a success rate of how often the task is accomplished in average, it can be the average speed of a swarm in collective motion etc. Here we are interested in the swarm performance as a function over 'swarm density' which is how many agents are found in average within a certain area. For the following reason the function of swarm performance depending on swarm density cannot simply be a linear function. For a true swarm scenario a very low density (e.g., corresponding to one agent in the whole area) has to result in low performance because there is neither cooperation nor a speed-up. With increasing density the performance increases because of a simple speed-up (e.g., two robots clean the floor faster than one) and because of increasing opportunities of cooperation (assuming that cooperation is an essential beneficial part of swarms). In natural swarms this performance increase with increasing swarm size is revealed in increased productivity and the emergence of increased division of labor as an indicator for increased cooperation (Jeanne and Nordheim, 1996; Karsai and Wenzel, 1998; Gautrais et al., 2002; Jeanson et al., 2007). Even a superlinear performance increase is possible in this interval (Mondada et al., 2005). At some critical/optimal density (Schneider-Fontán and Matarić, 1996) the performance curve will first level off and then decrease (Arkin et al., 1993) because improvements in cooperation possibilities will be lower than the drawback of high densities, namely interference (Lerman and Galstyan, 2002). With further increase of the density the performance continues to decrease (Goldberg and Matarić, 1997). Hence, swarms generally face a tradeoff between beneficial cooperation and obstructive interference. However, it is to be noted that interference has also positive effects both within certain swarms and as a tool for designing swarm algorithms (Dussutour et al., 2004; Goldberg and Matarić, 1997).

It turns out that not only these qualitative properties are similar in many swarm systems but also the actual shapes of swarm performance over swarm size/density graphs (see Fig. 2(a)). Examples are the performance of foraging in a group of robots (Fig. 2(b) and Fig. 10a in (Lerman and Galstyan, 2002)), the activation dynamics and information capacity in an abstract cellular automaton model of ants (Figs. 1b and 1c in (Miramontes, 1995)), and even in the sizes of social networks (Fig. 8b in (Strogatz, 2001)). A similar curve is also presented as a hypothesis for per capita output in social wasps by Jeanne and Nordheim (1996). Furthermore, notice that these shapes are typical in probability distributions such as Weibull, Wigner, and log-normal. The existence of this general shape was already reported by Østergaard et al. (2001) in their expected performance model for multi-robot systems in constrained environments:

> We know that by varying the implementation of a given task, we can move the point of "maximum performance" and we can change the shapes of the curve on either side of it, but we cannot change the general shape of the graph.

A related set of models are traffic models of flow over density. The 'fundamental diagram' of traffic flow (Lighthill and Whitham, 1955) is symmetric, more realistic models propose at least two asymmetric phases of free and synchronized flow. Actual measurements on highways show curves with shapes similar to Fig. 2(a) (e.g., see Fig. 6-4 in (Mahmassani et al., 2009)). In these models, there exist two densities for a given flow (except for maximum flow) similar to the situation here where we have two swarm densities for a given swarm performance.

1.2 Collective decisions

In the context of swarm intelligence, collective decision-making is a process that is distributed among a group of agents without global knowledge. Each agent decides based on locally sampled data such as the current decision of its neighbors. There are many biological systems showing collective decision-making, for example, food source choice in honey bees (Seeley et al., 1991), nest site selection in ants (Mallon et al., 2001), and escape route search in social spiders (Saffre et al., 1999). Collective decision-making systems are often modeled as positive-feedback systems that utilize initial fluctuations which are amplified and that way help to converge to a global decision (Deneubourg et al., 1990; Mallon et al., 2001; Nicolis et al., 2011). Interesting features of collective decisions are, for example, the speed-accuracy trade-off (Nicolis et al., 2011) or the influence of noise (Dussutour et al., 2009; Yates et al., 2009). Furthermore, it turns out that positive feedback is not always productive but can also generate irrational decisions (Nicolis et al., 2011).

In the following we limit our investigations to binary decision processes because they allow for a concise mathematical notation and hence allow an easy application of mathematical methods. The investigated systems are either inherently noisy (e.g., explicit stochastic processes within the agents' behaviors) or can validly modeled as noisy processes (e.g., deterministic chaos with strong dependence on the initial conditions). We are not interested in the quality of the final decision, that is the utility of choosing option A over option B or vice versa, and assume that there is no initial bias to one or the other. In selecting an appropriate model for collective decisions our main concern is simplicity while keeping attention on the relation of how much is needed as input to the model and how much is generated by it. We want to keep the number of parameters small while achieving descriptions of qualitative aspects of collective decisions as effects of the model. In order to obtain these standards we choose a minimal macroscopic model which has only one state variable describing the current status of the collective decision within the swarm (e.g., 80% for option A and consequently 20% for option B).

For simplicity we view the asynchronous distributed process of collective decisions as a round-based game which allows only one agent at a time to either revise its current decision or to convince a peer to revise its current decision. For this purpose we re-interpret well-known urn models as models of collective decisions and extend them appropriately. We use simple models inspired by the urn model of Ehrenfest and Ehrenfest (1907) and by the urn model of Eigen and Winkler (1993).

1.2.1 Ehrenfest urn model

This urn model was originally introduced by Ehrenfest and Ehrenfest (1907) in the context of dissipation, thermodynamics, statistical mechanics, and entropy. The dynamics of the model is defined as follows. Our urn is filled with N marbles. Say initially all marbles are blue. Whenever we draw a blue one, which is for sure in the first round, we replace it with a red marble. If we draw a red marble we replace it with a blue one. Obviously the two extreme states of either having an urn full of blue marbles or an urn full of red marbles are unstable. Similarly this is true for all states of unevenly distributed colors. To formalize this process we keep track of how the number of blue marbles (w.l.o.g.) changes depending on how many blue marbles were in the urn at that time. We can do this empirically or we can actually compute the average expected 'gain' in terms of blue marbles. For example, say at time t we have $B(t) = 16$ blue marbles in the urn and a total of $N = 64$ marbles. The probability of drawing a blue marble is therefore $P_B = \frac{16}{64} = 0.25$. The case of drawing a blue marble has to be weighted by -1 because that is the change in terms of blue marbles in that case. The probability of drawing a red marble is $P_R = \frac{48}{64} = 0.75$ which is weighted by $+1$. Hence, the expected average change ΔB of blue marbles per round depending on the current number of blue marbles $B = 16$ is $\Delta B(B = 16) = 0.25(-1) + 0.75(+1) = 0.5$. This can be done for all possible states yielding

$$\Delta B(B) = -2\frac{B}{64} + 1 \tag{1}$$

which is plotted in Fig. 1(a). Hence, the average dynamics of this game is given by $B(t + 1) = B(t) + \Delta B(B(t))$.

The recurrence $B_t = B_{t-1} + 1 - \frac{2}{64}B_{t-1}$ can be solved by generating functions (Graham et al., 1998). For $B_0 = 0$ we obtain the generating function

$$G(z) = \sum_t \left(\sum_{k \leq t} \left(\frac{62}{64} \right)^k \right) z^t \tag{2}$$

The tth coefficient $[z^t]$ of this power series is the closed form for B_t. We get

$$[z^t] = B_t = \sum_{k \leq t} \left(\frac{62}{64} \right)^k = \frac{1 - \left(\frac{62}{64}\right)^t}{1 - \frac{62}{64}}. \tag{3}$$

Hence, for initializations $B_0 = 0$ and the symmetrical case $B_0 = 64$ the system converges in average rather fast to the equilibrium $B = 32$. The actual dynamics of this game is, of course, a stochastic process which can, for example, be modeled by $B(t + 1) = B(t) + \Delta B(B(t)) + \xi(t)$, for a noise term ξ.

Several generalizations have been proposed for this urn model (Krafft and Schaefer, 1993; Klein, 1956), however, mostly these investigations were focused on mathematically tractable variants. In the following we report generalizations which are focused on applications to feedback processes.

1.2.2 Eigen urn model

The Ehrenfest model can be interpreted as an example of a negative feedback process. Deviations from the fixed point $B = 32$ are corrected by negative feedback (the predominant color will be diminished in average). Eigen and Winkler

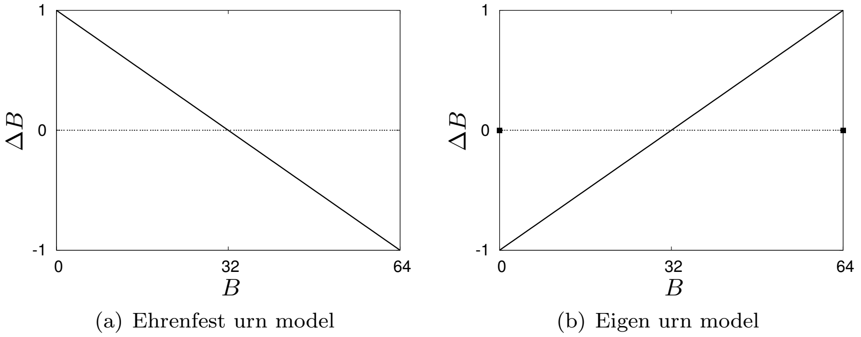

(a) Ehrenfest urn model (b) Eigen urn model

Figure 1: Expected average change in the urn models.

(1993) reported a similar urn model to show the effect of positive feedback. In this model drawing a blue marble has the effect of replacing a red marble by a blue one and vice versa. The expected average change of blue marbles per round changes accordingly to

$$\Delta B(B) = \begin{cases} 2\frac{B}{64} - 1, & \text{for } B \in [1, 63] \\ 0, & \text{else} \end{cases}, \tag{4}$$

for a plot see Fig. 1(b)

While we still have an expected change of $\Delta B = 0$ for $B = 32$ as in the Ehrenfest model, the fixed point $B = 32$ is unstable now as its surrounding drives trajectories away from $B = 32$ and towards the stable fixed points $B = 0$ and $B = 64$ respectively. In Sec. 3 we introduce a more general urn model that takes the intensity of positive feedback as a parameter and which can be used to model collective decisions in swarms.

2 Universal properties of swarm performance

Having identified the two main components (cooperation and interference) and the typical shape of these graphs we can define a simple model. The idea is to fit this model to empirical data for verification and predictions.

2.1 Simple model of swarm performance

For a given bounded, constant area A the swarm density ρ is defined by the swarm size N according to $\rho = N/A$. We define the swarm performance P depending on swarm size N by

$$P(N) = C(N)(I(N) - d) = a_1 N^b a_2 \exp(cN), \tag{5}$$

for parameters $c < 0$, $a_1, a_2, b > 0$, and $d \geq 0$ (see Fig. 2(a)). Parameter d is subtracted to force a decrease to zero ($\lim_{N\to\infty} I(N) - d = 0$). The swarm performance depends on two components C and I. First, the swarm effort without negative feedback is defined by the cooperation function (see also Fig. 2(a))

$$C(N) = a_1 N^b. \tag{6}$$

This function can be interpreted as the potential for cooperation in a swarm that would exist without certain constraints, such as physical collisions or other spatial restrictions. The same formula was used by Breder (1954) to model the cohesiveness of a fish school and by Bjerknes and Winfield (2010) to model swarm velocity in emergent taxis. However, they used parameters of $b < 1$ while we are using mostly values of $b > 1$. Second, the interference function (see also Fig. 2(a)) is defined by

$$I(N) = a_2 \exp(cN) + d, \tag{7}$$

with d used for scaling (e.g., $\lim_{N\to\infty} I(N) = d$). The interference function can also be interpreted as the swarm performance achievable without cooperation, that is, achievable swarm performance without positive feedback. The exponential decrease seems to be a reasonable choice, for example, compare Fig. 10b in (Lerman and Galstyan, 2002) which shows an exponentially decreasing efficiency per robot in a foraging task.

2.2 Examples

To prove the wide applicability of this simple model we fit it to some swarm performance plots that were available. We investigate four scenarios: foraging in a group of robots (Lerman and Galstyan, 2002), collective decision making (Hamann et al., 2012) based on BEECLUST (Schmickl and Hamann, 2011), aggregations in tree-like structures and reduction to shortest paths (Hamann, 2006) similar to (Hamann and Wörn, 2008), and the emergent taxis scenario (also sometimes called 'alpha algorithm', Nembrini et al. (2002); Bjerknes et al. (2007)).

Given the data of the overall performance, the four parameters of eq. 5 can be directly fitted. This was done for the first three of the four examples in Fig. 2. The equation can be well fitted to the empirical data. In case of the foraging scenario (Fig. 2(b)) we also have data of the efficiency per robot. We can use the model parameters, that were obtained by fitting the model to the overall performance, to predict the efficiency per robot which is a function that we suppose to be proportional to effects by interference. This is done by scaling the interference function linearly and plotting it against the efficiency per robot. The satisfying result is shown in Fig. 2(b).

We analyze the forth example, emergent taxis, in more detail. The following empirical data is based on a simple simulation. This simulation is noise-free and therefore robots move in straight lines except for u-turns according to the emergent taxis algorithm. First, we measure the performance that is achieved without cooperation. This is done by defining a random behavior that ignores any characteristic feature of the actual emergent taxis algorithm. For example, in the emergent taxis algorithm, robots count the number of neighbors and do

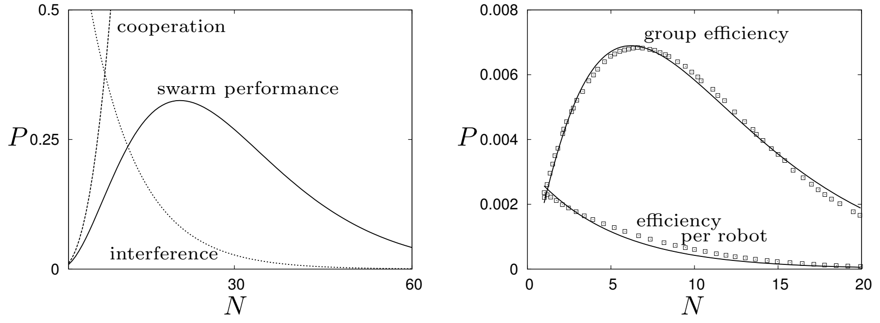

(a) Model of cooperation and interference, examples of swarm performance (eq. 5), cooperation (eq. 6), and interference (eq. 7) depending on swarm size.

(b) Foraging in a group of robots, eq. 5 fitted to group efficiency (upper solid line), prediction of interference (lower solid line, efficiency per robot, linearly rescaled), data points extracted from Fig. 10 in Lerman et al. (Lerman and Galstyan, 2002); P gives group/robot efficiency

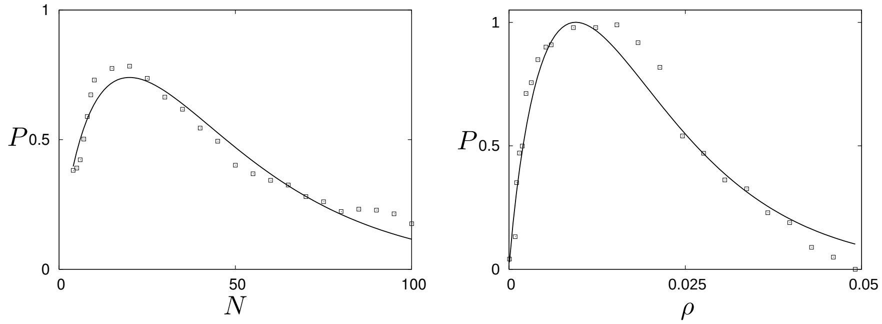

(c) Collective decision making (Hamann et al., 2012) based on BEECLUST (Schmickl and Hamann, 2011); values of $P = 1$ would indicate that 100% of the swarm have found a decision; $P = 0$ indicates symmetry between options

(d) Aggregation in tree-like structures and reduction to shortest path (Hamann, 2006); P gives the ratio of successful runs

Figure 2: Model of cooperation and interference and three scenarios with fitted performance P according to eq. 5

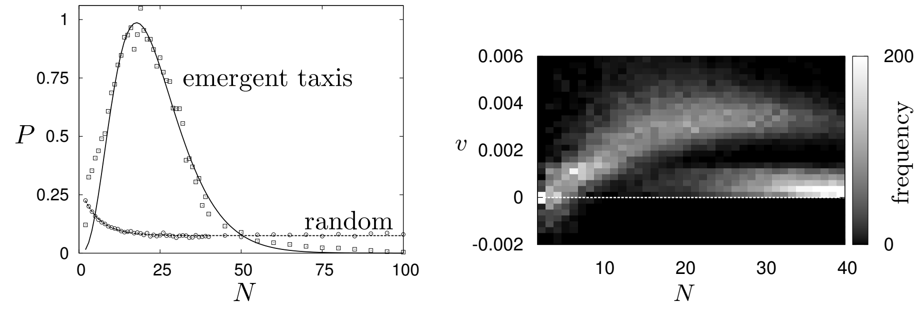

(a) Model fitted to data of random and emergent–taxis behavior; P is covered distance by barycenter times N.

(b) Histogram of barycenter speeds v for different swarm sizes. Note the bimodality about in the interval $N \in [16, 40]$.

Figure 3: Performance of a random behavior and the actual self-organized emergent taxis behavior (also sometimes called 'alpha algorithm') (Nembrini et al., 2002; Bjerknes et al., 2007) with fitted model (eq. 5); histogram showing two phases.

u-turns if this number drops below a threshold α. To obtain the cooperation-free behavior we have set this parameter to $\alpha = 0$ in the simulation. Hence, no robot will ever u-turn and they basically disperse in the arena. A simulation run is stopped once a robot touches a wall. The performance of the swarm P is measured by the total distance covered by the swarm's barycenter multiplied by the swarm size (i.e., an estimate of the sum of all distances that were effectively covered by each robot). The performance obtained by this random behavior can be fitted using the interference function of eq. 7 (interpreting the interference function as a measurement of swarm performance without cooperation). The well fitted interference function and the empirically obtained data is shown in Fig. 3(a) labeled 'random'. The bias towards the light source (positive covered distance) is due to the initial positioning of the swarm closer to the wall that is farther away from the light source. In a second step, we keep the interference function fixed and fit the full model of swarm performance P (eq. 5) to the data from the actual emergent taxis scenario by only varying the cooperation function (i.e., fitting a_1 and b while keeping a_2, c and d fixed). The fitted swarm performance model[1] is shown in Fig. 3(a) labeled 'emergent taxis'. This simple model is capable of predictions, if the interference function has been fitted and we fit the cooperation function only to a small interval of, for example, $N \in [20, 22]$ (i.e., intervals close to the maximal performance).

Note that we are working with a single averaged value to describe the performance which does not fully catch the system's behavior. At least in some scenarios, as here in the emergent taxis scenario, the performance does not just continuously decrease due to continuously increasing interference. Instead, two coexisting phases of behaviors emerge: functioning swarms moving forward and pinned swarms with extreme numbers of u-turns. In emergent taxis this is shown, for example, by a histogram of barycenter speeds in Fig. 3(b). For $N < 15$ the mean of a unimodal distribution increases with increasing N. Starting at about $N = 15$ a second phase emerges that shows slowly moving swarms and generates a bimodal distribution. Hence, given the fully deterministic implementation of our simulation, there are two classes of initial states (robot positions and orientations) that determine the two extremes of success or total failure. In other scenarios the interference might truly increase continuously due to a qualitatively different process, such as saturation of target areas with robots.

---

[1] Fitted parameters: $a_1 = 0.01061$, $b = 3.237$, $a_2 = 0.2138$, $c = -0.1823$, $d = 0.075$

3 Universal properties of collective decisions

In the following we investigate macroscopic models of collective decisions. One of the most general and at the same time simplest model of collective decisions is a model of only one state variable $s(t)$ which gives the temporal evolution of the swarm fraction that is in favor of one of the options in a binary decision process. If we assume that there is no initial bias to either option (i.e., full symmetry), then we need a tie breaker for $s = 0.5$. A good choice for a tie breaker is noise because any real swarm will be noisy. The average change of s depending on itself per time ($\Delta s(s)/\Delta t$) is of interest. Given that the system should be able to converge to either of the options at a time plus having the symmetric case of $s = 0.5$ we end up with at least three zeros for $\Delta s(s)/\Delta t$ and consequently at least a cubic function. Instead of developing a model, that defines such a function, we prefer a model that allows this function to emerge from a simple process. In swarms the tendency to a certain option once symmetry is overcome (say, for $s = 0.5 + \epsilon$ towards $s = 1$) is typically a result of positive feedback. We define such a process depending on probabilities of positive feedback next.

3.1 Simple model of collective decisions

As discussed in the introduction we define an urn model that was inspired by the models of Ehrenfest and Ehrenfest (1907) and of Eigen and Winkler (1993). Here we use an urn model that has optionally positive or negative feedback depending on the system's current state and depending on a stochastic process. The urn is filled with N marbles which are either red or blue. The game's dynamics is turn-based. First a marble is drawn with replacement followed by replacing a second one determined by the color of the first marble. The probability of drawing a blue marble is implicitly determined by the current number of blue marbles $B(t)$ in the urn. The subsequent replacement of a second marble effects either a positive or a negative feedback. The feedback is determined explicitly by a probability $P(s, \varphi)$ that is based on the current ratio s of either the blue marbles in the urn or the ratio of red marbles. For now we choose a sine function

$$P(s, \varphi) = \varphi \sin(\pi s). \tag{8}$$

Due to the symmetry $P(s,\varphi) = P(1-s,\varphi)$ it is irrelevant whether s is set to the ratio of blue marbles or the ratio of red marbles. Later we will find that similar but different functions might be a better choice in certain situations (Sec. 3.4). The constant $\varphi \in [0,1]$ scales the amplitude of the sine function (see Fig. 6(a)) and consequently defines the predominant 'sign' and the probabilities of positive and negative feedback. The integral $\int_0^1 P(s,\varphi)ds$ gives the overall probability of having positive feedback independent of s. For $\varphi < 0.5$ negative feedback is predominant for any s and for $\varphi > 0.5$ an interval around $s = 0.5$ emerges for which positive feedback is predominant.

Say we draw a blue marble, we notice the color, and put it back into the urn. Then our model defines that with probability $P(s(t),\varphi)$ a red marble will be replaced by a blue one (i.e., a positive feedback event because drawing a blue one increased the number of blue marbles) and with probability $1 - P(s(t),\varphi)$ a blue one will be replaced by a red one (i.e., a negative feedback event because now drawing a blue one decreased the number of blue marbles). Hence, the probability $P(s,\varphi)$ gives the probability of positive feedback. $P(s,\varphi)$ is plotted for different settings of φ in Fig. 6(a). There is maximum probability for positive feedback for the fully symmetric case of $s = 0.5$ as clearly seen in Fig. 6(a). For $s = 0$ and $s = 1$ we have $P(s,\varphi) = 0$ because no positive feedback is possible (either all marbles are already blue or all marbles are red and therefore no blue one can be drawn). For $\varphi \leq 0.5$ the probability of positive feedback is small ($\varphi \leq 0.5, \forall s : P(s,\varphi) \leq 0.5$), consequently the system is stable and kept around $s = 0.5$.

The analogy of this model to a collective decision making scenario is the following. The initial drawing resembles the frequency of individual decisions in the swarm over time proportional to s within the turn-based model. Consequently we serialize the system dynamics and each system state $B(t)$ has at most two predecessors ($B(t-1) = B(t) \pm 1$). The replacement of the second marble resembles the effect of either a swarm member convincing another one about its decision or being convinced of the opposite.

Based on the above definitions the average expected change per round ΔB of blue marbles B can be calculated by summing over the four cases: drawing a blue or red marble, followed by positive or negative feedback, multiplied by the 'payoff' in terms of blue marbles respectively. Using the symmetry $P(s,\varphi) = P(1-s,\varphi)$ we get

$$\begin{aligned}\Delta B(s) = \quad & sP(s,\varphi)(+1) + s(1-P(s,\varphi))(-1) \\ & + (1-s)P(1-s,\varphi)(-1) + (1-s)(1-P(1-s,\varphi))(+1) \\ = \quad & 4(P(s,\varphi) - 0.5)(s - 0.5). \qquad (9)\end{aligned}$$

We defined $P(s,\varphi)$ based on a trigonometric function but alternatively one can choose, for example, a quadratic function

$$P(s,\varphi) = \varphi(1 - 4(s-0.5)^2) \qquad (10)$$

yielding a cubic function

$$\Delta B(s) = 2(s-0.5) - 16(s-0.5)^3. \qquad (11)$$

Also note that by turning positive feedback completely off ($P(s) = 0$) we obtain the Ehrenfest urn model again (cf. eqs. 1 and 9) and by activating maximal positive feedback ($P(s) = 1$) we obtain the Eigen urn model (cf. eq. 4).

While in the above definition the positive feedback probability $P(s, \varphi)$ is explicitly given, it might be unknown in applications of this model. In these applications the positive feedback itself might not be measurable but maybe the number of observed decision revisions of the agents. We introduce the absolute number of observed individual decision revisions from red to blue $r_b(s)$ over any given period and from blue to red $r_r(s)$. The ratio of red-to-blue revisions is directly related to the expected average change per round

$$\frac{r_b(s)}{r_b(s) + r_r(s)} = 0.5(\Delta B(s) + 1). \tag{12}$$

Based on $\frac{r_b(s)}{r_b(s)+r_r(s)}$ and by considering the above mentioned four cases (drawing a blue or red marble, followed by positive or negative feedback) the following equation holds for red-to-blue revisions

$$P(s)s + (1 - P(1 - s))(1 - s) = \frac{r_b(s)}{r_b(s) + r_r(s)}, \tag{13}$$

which yields (using symmetries)

$$P(s) = \frac{\frac{r_b(s)}{r_b(s)+r_r(s)} - 1 + s}{2s - 1}, \text{ for } s \neq 0.5, \frac{r_b(s)}{r_b(s) + r_r(s)} \leq \max(s, 1 - s), \tag{14}$$

an equation which is to be used to determine the positive feedback probability based on measurements of agents' revisions. The pole at $s = 0.5$ and the consequently undefined $P(s = 0.5)$ is reasonable. Any definition of $P(s = 0.5)$ would be without effect to the system because negative and positive feedback are indistinguishable at $s = 0.5$. We actually define $P(s = 0.5)$ in eq. 8, which is however only a simplification of notation. Also note that this mathematical difficulty has limited effect in applications because swarms are inherently discrete. For example, the exact $s = 0.5$ does not exist for odd swarm sizes. The squares in Fig. 6(a) give the redetermined $P(s)$ based on eq. 14 and on measurements of $r_b(s)$ and $r_r(s)$. The values for $P(s = 0.5)$ cannot be given, as discussed, and also values in the vicinity of $s = 0.5$ show discrepancies because they are close to the pole of eq. 14.

In Fig. 6(b) we compare the theoretical average change per round ΔB according to eq. 9 to the empirically obtained average change $\overline{\Delta B}$ in terms of number of marbles for the different settings of φ. The agreement between theory and empiric data is close to perfect as expected. Two zeros s_1 and s_2 emerge additionally to $s_0 = 0.5$ for $\varphi > 0.5$: $s_1 = \frac{1}{\pi} \arcsin(\frac{1}{2\varphi})$ and $s_2 = 1 - \frac{1}{\pi} \arcsin(\frac{1}{2\varphi})$. Positive values of $\Delta B(s)$ for $s < 0.5$ represent dynamics that has a bias towards $s = 0.5$ and negative values represent dynamics with a bias towards $s = 0$ and vice versa for the other half ($s > 0.5$).

Fig. 6(c) gives an estimate of the asymptotic behavior of this urn model for varied feedback intensity φ. It shows a pitchfork bifurcation at $\varphi = 0.5$ which is to be expected based on Fig. 6(b) and which is fuzzy because it is a stochastic process. For $\varphi > 0.5$ the curve defined by $\Delta B(s)$ becomes cubic and generates two new stable fixed points while the former at $s = 0.5$ becomes unstable.

3.2 Optional extension of the model

Since positive and negative feedback is determined stochastically based on the current global state in the urn model, it is straight forward to determine the number of replaced marbles stochastically, too. Instead of having a fixed 'payoff' (number of replaced marbles) of ± 1 we can, for example, define a probability M of the event 'having a payoff of ± 1' and a probability $1 - M$ for a payoff of 0. Thus the average payoff would be $\pm M$. In addition, the payoff can be variant depending on the current global state s, that is, we define a function $M(s)$. It turns out that a definition similar to the positive feedback probability $P(s, \varphi)$ is useful

$$M(s) = c_1 \sin(\pi s) + c_2, \tag{15}$$

for appropriately chosen constants c_1 and c_2. $M(s)$ defines the average over absolute values of changes in s, similar to the diffusion coefficient in Fokker-Planck theory. Measurements of the diffusion coefficient in swarm systems were reported in (Yates et al., 2009; Hamann et al., 2010) which show low values for $s \ll 0.5$ and $s \gg 0.5$ with a peak at $s = 0.5$. With $M(s)$ defined by eq. 15 we have symmetry again ($M(s) = M(1 - s)$) and hence the extension of eq. 9 is simply

$$\Delta B(s) = 4M(s)(P(s, \varphi) - 0.5)(s - 0.5). \tag{16}$$

3.3 Available and unavailable methods

Note that the recurrence $B_t = B_{t-1} + \Delta B(B_{t-1})$ is a trigonometric or cubic function based on eq. 8 or eq. 10 respectively. Thus, it is much more difficult to be analytically handled and a concise result as for the Ehrenfest model (eq. 3) cannot be obtained. When applying nonlinear equations for ΔB we enter the domains of nonlinear dynamics and chaotic systems with all their known mathematical intractabilities. Hence, in general we have to rely on numerical methods.

However, if we choose to investigate probability distributions $\rho(s, t)$ instead of single trajectories $s(t)$, an interesting mathematical option is available. The steady state $\pi(s)$ of the probability distribution $\rho(s, t)$ over an ensemble of realizations of $s(t)$ can be obtained analytically. We assume for simplicity that the current state of the collective decision system changes every step by exactly one marble. The process defined by the urn model is memoryless, that is, it has Markov property and we can define a Markov chain with $N + 1$ states. We define the transition matrix $\mathbf{T}$ of the Markov chain by

$$\begin{aligned} T_{2,1} &= \frac{1}{2}\left(\Delta B\left(\frac{0}{N}\right)+1\right), && \\ T_{i+1,i} &= \frac{1}{2}\left(\Delta B\left(\frac{i-1}{N}\right)+1\right), && \text{for } i \in [2,N], \\ T_{i-1,i} &= 1-\frac{1}{2}\left(\Delta B\left(\frac{i-1}{N}\right)+1\right), && \text{for } i \in [2,N], \\ T_{N,N+1} &= 1-\frac{1}{2}\left(\Delta B\left(\frac{N}{N}\right)+1\right). && \end{aligned} \tag{17}$$

The steady state is then computed by determining the eigenvectors $\mathbf{v}$

$$\mathbf{T}\mathbf{v} = \lambda\mathbf{v}. \tag{18}$$

Generally there are several eigenvectors but only one that has no changing sign in its elements (all positive or all negative) which represents the equilibrium distribution of the Markov chain π or $-\pi$ respectively.

With the steady state at hand, several methods of statistical analysis are available. For example, we can calculate splitting probabilities (Gardiner, 1985). The splitting probability $\sigma_{a,b}(x)$ gives the probability that the system initialized at $s = x$ will reach the state $s = b$ before the state $s = a$. It is calculated by

$$\sigma_{a,b}(x) = \int_a^x \pi(s)^{-1} ds \left(\int_a^b \pi(s)^{-1} ds\right)^{-1}. \tag{19}$$

We set a and b to the positions of the two peaks in the steady state probability density π that we obtain for $\varphi = 1$. Results for varied positive feedback intensity φ (while keeping a and b constant) are shown in Fig. 4. It is clearly seen that for $\varphi < 0.5$ there is a wide interval with a fifty-fifty chance to end at either of the two peaks. Beginning with $\varphi = 0.5$ and with increasing φ the probability of switching from one peak to the other is decreasing considerably which is an indicator for an effective collective decision.

Another statistical property of Markov processes, especially those with bistable potentials, is the mean first passage time. Of interest is the mean time to switch from the collective decision for option A ($s = s_1$ with $\Delta B(s_1) = 0$) to option B ($s = s_2$ with $\Delta B(s_2) = 0$). The switching time is of particular interest in the context of swarm intelligence because it tells whether a swarm is able to stay for a considerable time in a given state (e.g., see Yates et al. (2009)). In case of collective motion the mean switching time describes whether the swarm will be aligned long enough to cover a considerable distance.

Markov theory allows to calculate the mean first passage time using the transition matrix $\mathbf{T}$ and specifying a target state i which is defined to be absorbing ($T_{i,i} = 1$), that is, we convert the system into an absorbing Markov chain. Using the fundamental matrix $\mathbf{M} = (\mathbf{I} - \mathbf{Q})^{-1}$ (with identity matrix $\mathbf{I}$

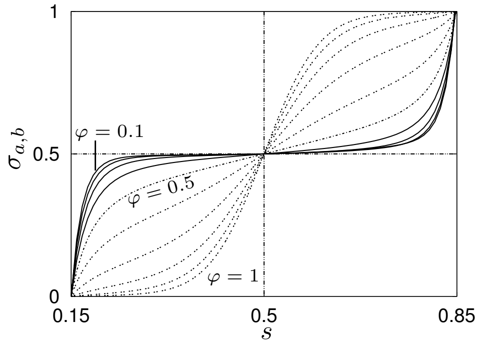

Figure 4: Splitting probabilities $\sigma_{a,b}$ between the two peaks in the steady state probability density π for varied positive feedback intensity $\varphi \in \{0.1, 0.2, \ldots, 1\}$.

and $\mathbf{Q}$ is the transition matrix of transitional states) a vector of mean first passage times for all transitional states is obtained by $\mathbf{Mc}$ with $\mathbf{c}$ is a column vector of all 1's, see Grinstead and Snell (1997). In addition an estimate of the mean switching time can be determined numerically in the urn model by generating trajectories $s(t)$ and observing the switching behavior. This estimate is a lower bound (finite simulation time, finite number of samples, power-law distribution of first passage times). A comparison between theory and simulation along with fitted functions $(a \exp(bN)(cN)^d)$ is shown in Fig. 5. The switching time scales approximately exponentially with swarm size N.

3.4 Examples

Next we want to compare the data from our urn model (Fig. 6(b)) to data from more complex models, such as the density classification scenario (Hamann and Wörn, 2007). In the following we apply the more general definition of ΔB (eq. 16) but with an invariant payoff $M(s) = c$ for a scaling constant c that scales the average change for different payoffs.

The density classification scenario (Hamann and Wörn, 2007) is about a swarm of red and green agents moving around randomly. Their only interaction is constantly keeping track of those agents' colors they bump into. Once an agent has seen five agents of either color it changes its own color to that it has encountered most. Here, s gives the ratio of red agents. The name of this scenario is due to the idea that the swarm should converge to that color that was initially superior in numbers. It turns out that the averaged change $\overline{\Delta s(s)/\Delta t}$ (see Fig. 6(d)) starts with a curve similar to that of $\varphi = 0$ in Fig. 6(b) and then converges to a curve that is similar to that of $\varphi = 0.75$. That is, $\overline{\Delta s(s)/\Delta t}$ is time-variant and, for example, the above mentioned Markov model would have to be extended to a time-inhomogeneous Markov model to achieve a better correlation with the measurements. Early in the simulation there is mostly negative feedback forcing values close to $s = 0.5$. With increasing time the negative

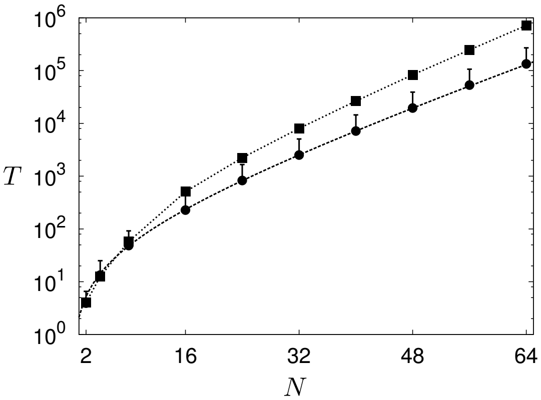

Figure 5: Mean first passage times T between the two collective decisions s_1 and s_2 with $\Delta B(s_1) = \Delta B(s_2) = 0$ over swarm size N, squares give values according to Markov theory, circles give measurements of the urn model, error bars give standard deviations, lines are fitted functions $a \exp(bN) N^d$.

feedback decreases which results finally in positive feedback for $s \in [0.23, 0.77]$. Comparing Fig. 6(b) to Fig. 6(d) indicates a good qualitative agreement between our urn model and the density classification scenario. Given that the curves in Fig. 6(d) converge over time to the final shape which is resembled by our model for increasing φ in Fig. 6(b), one can say that positive feedback builds up slowly over time in the density classification scenario. By fitting eq. 16 to the data shown in Fig. 6(d) we get estimates for the feedback intensity φ. From the earliest and steepest line to the latest and only curve with positive slope in $s = 0.5$ we get values of $\varphi \in [0, 0, 0, 0.007, 0.304, 0.603]$ for times $t \in [100, 200, 400, 800, 1600, 3200]$. By continuing this fitting for additional data not shown in Fig. 6(d), we are able to investigate the temporal evolution of feedback intensity φ according to our model. In Fig. 6(e), the data points of feedback intensity φ obtained by fitting are shown along with a function that was fitted to the data. This result supports the assumption of a 'negative exponential' increase over time $(1 - \exp(-t))$ of positive feedback in this system as already stated in (Hamann et al., 2010).

The positive feedback probability $P(s)$ can also be measured via the observed decision revisions according to eq. 14. This was done for the density classification scenario; the results are given in Fig. 7(a) which shows the measured positive feedback probability $P(s)$ for time $t = 7900$. The data was fitted using the following axially symmetric function

$$P(s) = \begin{cases} c_1 \left(1 - \frac{1}{1+c_2 s}\right), & \text{for } s \leq 0.5 \\ c_1 \left(1 - \frac{1}{1+c_2(1-s)}\right), & \text{else} \end{cases}, \tag{20}$$

for constants c_1 and c_2, which turns out to be a better fit here than the sine function. Once the function is fitted it can be used to calculate the expected average change Δs following eq. 16 (only scaling constant c needs to be fitted). As seen in Fig. 7(b) we obtain a very good fit. Indeed our experience shows that the procedure of fitting $P(s)$ instead of Δs directly is much more accurate and needs fewer samples. Especially it places the zeros $\Delta s = 0$ more accurate which are important to predict the correct steady state of the system. Even with just 100 samples good fits were obtained which indicates that this model could be applied to data from natural swarm systems. The prediction of the steady state based on the measured positive feedback probability following eqs. 16, 17, and 18 is shown in Fig. 7(c). In comparison to the measurements from simulation this prediction shows a reasonable agreement.

Other examples showing similarities to the $\varphi = 0.75$-graph in Fig. 6(b) are Figs. 2B and 3B in Yates et al. (2009) which show the drift coefficient dependent on the current alignment of a swarm (average velocity). While the data obtained from experiments with locusts, Fig. 2B in (Yates et al., 2009), is too noisy, we use the data from their model, Fig. 3B in (Yates et al., 2009), to fit our model. The result is shown in Fig. 6(f). We obtain a maximal positive feedback of $\varphi = 1$.

4 Discussion and Conclusion

We have reported two abstract swarm models with high generality due to our long-term objective of creating a swarm calculus. The first model describes the dependency of swarm performance on swarm density by separation into two parts: cooperation and interference. It explains the existence of an optimal or critical swarm density at which the peak performance is reached. The second model describes the dynamics of collective decision processes based on the existence and intensity of feedback. It explains how the cubic functions of decision revision emerge by an increase of positive feedback over time.

The first model is simple and the existence of optimal swarm densities is well known. However, to the authors knowledge, no similar model combined with a validation by fitting the model to data from diverse swarm applications was reported before except for the hypotheses stated by Østergaard et al. (2001). Despite its simplicity the model has the capability to give predictions of swarm performance, especially, if the available data, to which it is fitted, includes an interval around the optimal density. That way this model might serve as a swarm calculus of swarm performance. In addition, we want to draw attention to the problem of masking special density-dependent properties by only investigating the mean performance. The example shown in Fig. 3(b) documents the existence of phases in swarm systems.

The second model is also abstract but has a higher complexity and is more conclusive because it allows for mathematical derivations. Based on our urn model for positive feedback decision processes the emerging cubic function of decision revision can be derived (see eq. 9). Hence, we generate the function of decision revision based on our urn model which allows for an interpretation of how the function emerges while, for example, in (Yates et al., 2009) this function is measured in a local model. Our model of collective decisions might qualify as

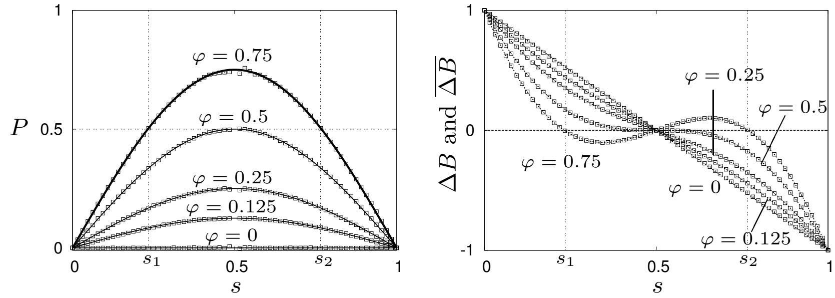

(a) Examples of setting the probability of positive feedback for intensities of feedback $\varphi \in \{0, 0.125, 0.25, 0.5, 0.75\}$, squares give the redetermined values according to eq. 14.

(b) Average change of $B(t)$ in terms of marbles, lines according to eq. 9, squares give empirical data, number of samples is 8×10^5 for each possible s, 64 marbles.

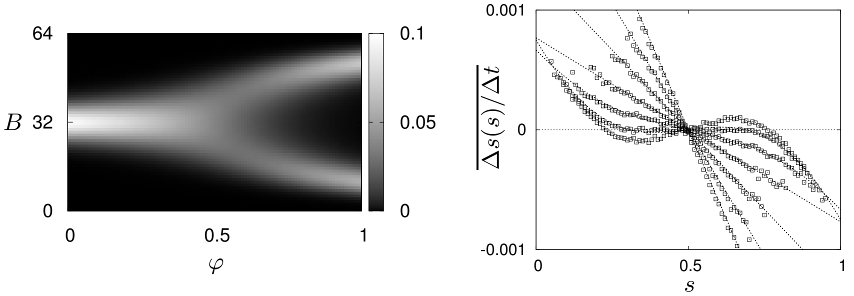

(c) Normalized histogram of blue marbles B over intensity of feedback φ after $t = 200$ steps, initialized to $B(0) \in \{32, 33\}$, indicating a pitchfork bifurcation at $\varphi = 0.5$.

(d) Density classification scenario (Hamann and Wörn, 2007), change of the ratio of red robots for different times during simulation, squares give empirical data (from (Hamann et al., 2010)), lines are fitted according to eq. 16.

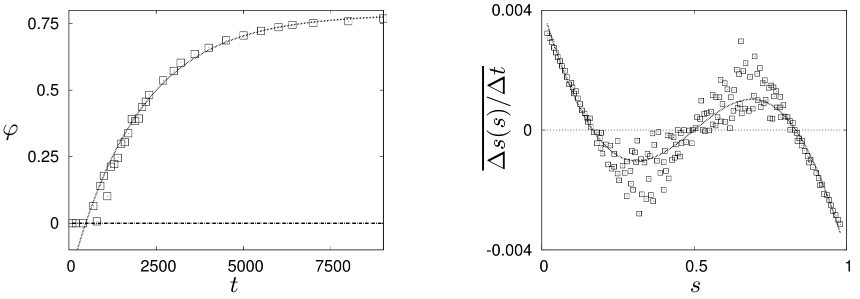

(e) Negative exponential function $\varphi(t) = 0.786 - \exp(-5 \times 10^{-4}t)$ fitted to feedback intensities obtained from the density classification scenario.

(f) Model fitted to data from Fig. 3B of Yates et al. (2009) (local model of swarm alignment in locusts) by $\varphi = 1$ (and $c = 4.134 \times 10^{-3}$); data scaled to $s \in [0, 1]$.

Figure 6: Settings of the positive feedback probabilities, resulting average change in $B(t)$ in the urn model over the ratio of marbles s, histogram of blue marbles for varied intensity of feedback φ, comparison of model and results from the density classification scenario (Hamann and Wörn, 2007), increase of positive feedback over time, and comparison of model and results from Yates et al. (2009).

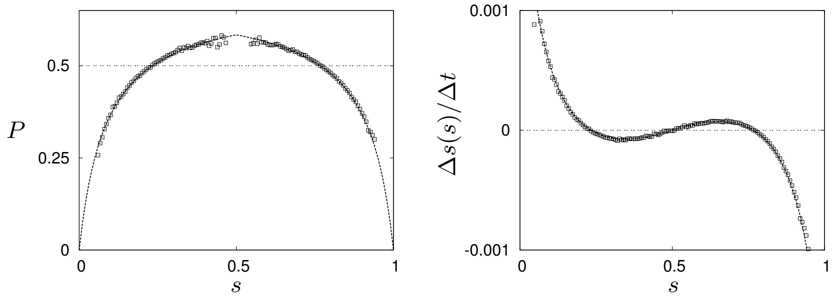

(a) Positive feedback probability as measured in the simulation according to eq. 14 (squares) and fitted function of eq. 20 (line).

(b) Predicted average change based on the measurements shown in (a) and eq. 16 (line) compared to direct measurements in simulation (squares).

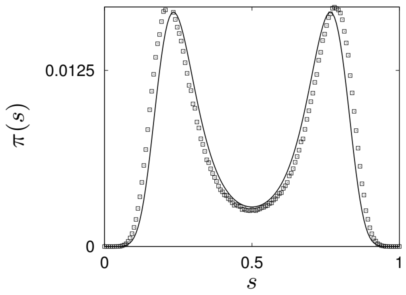

(c) Predicted steady state obtained by using the measurements shown in (a) and by applying eqs. 16, 17, and 18 (line); direct measurement in simulation (squares).

Figure 7: Measured positive feedback probability, predicted and measured average change Δs, and predicted and measured steady state for the density classification scenario.

a part of swarm calculus because those decision revision functions seem to be a general phenomenon in swarms.

This model can also be used to predict probability density functions of steady states in swarm systems. The workflow of measuring the positive feedback probability $P(s)$, fitting a function, using this function to calculate the expected average change Δs, which can in turn be used to predict the expected probability density function of the steady state (eigenvectors of transition matrix), is accurate with comparatively small sample numbers.

A model of notable similarity was published in the context of 'sociophysics' (Galam, 2004). It is based on the assumption that subgroups form in collective decisions within which a majority rule determines the subgroup's decision. The addition of contrarians, that is voters always voting against the current majority decision, generates dynamics that are similar to the reported observations in noisy swarms. Galam's model is, however, focused on constant sizes of these subgroups and their combinatorics while in swarm intelligence these groups and their sizes are dynamic.

An interesting result is also the particular function of the positive feedback increase over time $(1-\exp(-t))$ in the density classification task (see Fig. 6(e)). Note that this increase seems to be independent from respective values of s. Furthermore, values close to the bounds ($s \approx 1$ or $s \approx 0$) are not observed. An investigation of the underlying processes is beyond this paper but we want to state two ideas. First, the final saturation phase ($\lim_{t\to\infty} \varphi = 0.8$) is most likely caused by explicit noise in the simulation. The agent–agent recognition rate was set to 0.8 which keeps $P(s, \varphi)$ small. Second, the initial fast increase of φ (after a transient which might also be caused by the simulation because agents revise their color only after a minimum of five agent–agent encounters) might be caused by locally emerging sub-groups of homogeneous color within small areas that generate 'islands' of early positive feedback. These properties might, however, be highly stochastic and difficult to measure. Time-variant positive feedback was also observed in BEECLUST-controlled swarms as reported before (Hamann et al., 2012). Hence, a feedback system as given in Fig. 8 seems to be a rather common situation in swarm systems. In terms of the above urn model we can mimic this situation by saying A in Fig. 8 is the number of blue marbles (w.l.o.g.), B is the probability of drawing a blue marble, P is the probability of positive feedback (i.e., this edge can also negatively influence A), and C is an unspecified state variable that increases positive feedback (φ) over time and is influenced by an additional, unknown process. This triggers the question of what C can be and how it influences the feedback process independent of the current swarm consensus s.

We get maximally positive feedback $\varphi = 1$ for the data of Yates et al. (2009) as seen in Fig. 6(f) with the effect that situations of low alignment ($s \approx 0.5$) are left as fast as possible. This reinforces the findings of Yates et al. (2009) about the diffusion coefficient. A major feature of the self-organizing processes in the swarm seems to be that times in states of low alignment are minimized by the system (Yates et al.: "A higher diffusion coefficient at lower alignments suggests that the locusts 'prefer' to be in a highly aligned state").

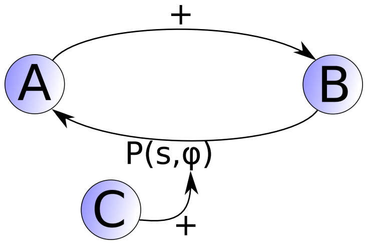

Figure 8: Time-variant feedback system; here for increasing probability of positive feedback.

The result of this paper is that generally applicable swarm models, that have simple preconditions, exist. To apply the model of swarm performance, only a concept of swarm density is necessary and to apply the model of collective decisions only a consensus variable of a binary decision is necessary. Despite their simplicity, both models have enough explanatory power to give insights into swarm processes such as the interplay of cooperation and interference and the installation of positive feedback. Hence, we contend that it is possible to generate a set of models and methods of general applicability for swarm science, that is, to create a swarm calculus.

References

Arkin, R. C., Balch, T., and Nitz, E. (1993). Communication of behavorial state in multi-agent retrieval tasks. In *Proc. IEEE Conf. on Robotics and Automation*, pages 588–594. IEEE Press.

Berman, S., Kumar, V., and Nagpal, R. (2011). Design of control policies for spatially inhomogeneous robot swarms with application to commercial pollination. In *IEEE International Conference on Robotics and Automation (ICRA'11)*, pages 378–385.

Bjerknes, J. D. and Winfield, A. (2010). On fault-tolerance and scalability of swarm robotic systems. In *Proc. Distributed Autonomous Robotic Systems (DARS 2010)*.

Bjerknes, J. D., Winfield, A., and Melhuish, C. (2007). An analysis of emergent taxis in a wireless connected swarm of mobile robots. In *IEEE Swarm Intelligence Symposium*, pages 45–52, Los Alamitos, CA. IEEE Press.

Breder, C. M. (1954). Equations descriptive of fish schools and other animal aggregations. *Ecology*, 35(3):361–370.

Camazine, S., Deneubourg, J.-L., Franks, N. R., Sneyd, J., Theraulaz, G., and Bonabeau, E. (2001). *Self-Organizing Biological Systems*. Princeton Univ. Press.

Deneubourg, J.-L., Aron, S., Goss, S., and Pasteels, J. M. (1990). The self-organizing exploratory pattern of the argentine ant. *Journal of Insect Behavior*, 3(2):159–168.

Dussutour, A., Beekman, M., Nicolis, S. C., and Meyer, B. (2009). Noise improves collective decision-making by ants in dynamic environments. *Proceedings of the Royal Society London B*, 276:4353–4361.

Dussutour, A., Fourcassié, V., Helbing, D., and Deneubourg, J.-L. (2004). Optimal traffic organization in ants under crowded conditions. *Nature*, 428:70–73.

Edelstein-Keshet, L. (2006). Mathematical models of swarming and social aggregation. *Robotica*, 24(3):315–324.

Ehrenfest, P. and Ehrenfest, T. (1907). Über zwei bekannte Einwände gegen das Boltzmannsche H-Theorem. *Physikalische Zeitschrift*, 8:311–314.

Eigen, M. and Winkler, R. (1993). *Laws of the game: how the principles of nature govern chance*. Princeton University Press.

Galam, S. (2004). Contrarian deterministic effect: the "hung elections scenario". *Physica A*, 333:453–460.

Gardiner, C. W. (1985). *Handbook of Stochastic Methods for Physics, Chemistry and the Natural Sciences*. Springer-Verlag.

Gautrais, J., Theraulaz, G., Deneubourg, J.-L., and Anderson, C. (2002). Emergent polyethism as a consequence of increased colony size in insect societies. *Journal of Theoretical Biology*, 215(3):363–373.

Goldberg, D. and Matarić, M. J. (1997). Interference as a tool for designing and evaluating multi-robot controllers. In *Proc. of the national conference on artificial intellgince (AAAI'97)*, pages 637–642.

Graham, R., Knuth, D., and Patashnik, O. (1998). *Concrete Mathematics: A Foundation for Computer Science*. Addison–Wesley.

Grinstead, C. M. and Snell, J. L. (1997). *Introduction to Probability*. American Mathematical Society.

Hamann, H. (2006). Modeling and investigation of robot swarms. Master's thesis, University of Stuttgart, Germany.

Hamann, H. (2010). *Space-Time Continuous Models of Swarm Robotics Systems: Supporting Global-to-Local Programming*. Springer-Verlag.

Hamann, H., Meyer, B., Schmickl, T., and Crailsheim, K. (2010). A model of symmetry breaking in collective decision-making. In Doncieux, S., Girard, B., Guillot, A., Hallam, J., Meyer, J. A., and Mouret, J. B., editors, *From Animals to Animats 11*, volume 6226 of *LNAI*, pages 639–648. Springer-Verlag.

Hamann, H., Schmickl, T., Wörn, H., and Crailsheim, K. (2012). Analysis of emergent symmetry breaking in collective decision making. *Neural Computing & Applications*, 21(2):207–218.

Hamann, H. and Wörn, H. (2007). Embodied computation. *Parallel Processing Letters*, 17(3):287–298.

Hamann, H. and Wörn, H. (2008). Aggregating robots compute: An adaptive heuristic for the Euclidean Steiner tree problem. In *The tenth International Conference on Simulation of Adaptive Behavior (SAB'08)*, volume 5040 of *LNAI*, pages 447–456. Springer-Verlag.

Jeanne, R. L. and Nordheim, E. V. (1996). Productivity in a social wasp: per capita output increases with swarm size. *Behavioral Ecology*, 7(1):43–48.

Jeanson, R., Fewell, J. H., Gorelick, R., and Bertram, S. M. (2007). Emergence of increased division of labor as a function of group size. *Behav. Ecol. Sociobiol.*, 62:289–298.

Karsai, I. and Wenzel, J. W. (1998). Productivity, individual-level and colony-level flexibility, and organization of work as consequences of colony size. *Proc. Natl. Acad. Sci. USA*, 95:8665–8669.

Klein, M. J. (1956). Generalization of the Ehrenfest urn model. *Physical Review*, 103(1):17–20.

Krafft, O. and Schaefer, M. (1993). Mean passage times for triangular transition matrices and a two parameter Ehrenfest urn model. *Journal of Applied Probability*, 30(4):964–970.

Lerman, K. and Galstyan, A. (2002). Mathematical model of foraging in a group of robots: Effect of interference. *Autonomous Robots*, 13:127–141.

Lerman, K., Martinoli, A., and Galstyan, A. (2005). A review of probabilistic macroscopic models for swarm robotic systems. In Şahin, E. and Spears, W. M., editors, *Swarm Robotics - SAB 2004 International Workshop*, volume 3342 of *Lecture Notes in Computer Science*, pages 143–152. Springer-Verlag.

Lighthill, M. J. and Whitham, G. B. (1955). On kinematic waves. II. A theory of traffic flow on long crowded roads. *Proceedings of the Royal Society of London*, A229(1178):317–345.

Mahmassani, H. S., Dong, J., Kim, J., Chen, R. B., and Park, B. (2009). Incorporating weather impacts in traffic estimation and prediction systems. Technical Report FHWA-JPO-09-065, U.S. Department of Transportation.

Mallon, E. B., Pratt, S. C., and Franks, N. R. (2001). Individual and collective decision-making during nest site selection by the ant *leptothorax albipennis*. *Behav. Ecol. Sociobiol.*, 50:352–359.

Milutinovic, D. and Lima, P. (2007). *Cells and Robots: Modeling and Control of Large-Size Agent Populations*. Springer-Verlag.

Miramontes, O. (1995). Order-disorder transitions in the behavior of ant societies. *Complexity*, 1(1):56–60.

Mondada, F., Bonani, M., Guignard, A., Magnenat, S., Studer, C., and Floreano, D. (2005). Superlinear physical performances in a SWARM-BOT. In Capcarrere, M. S., editor, *Proc. of the 8th European Conference on Artificial Life (ECAL)*, volume 3630 of *Lecture Notes in Computer Science*, pages 282–291. Springer-Verlag.

Nembrini, J., Winfield, A. F. T., and Melhuish, C. (2002). Minimalist coherent swarming of wireless networked autonomous mobile robots. In Hallam, B., Floreano, D., Hallam, J., Hayes, G., and Meyer, J.-A., editors, *Proceedings of the seventh international conference on simulation of adaptive behavior on From animals to animats*, pages 373–382, Cambridge, MA, USA. MIT Press.

Nicolis, S. C., Zabzina, N., Latty, T., and Sumpter, D. J. T. (2011). Collective irrationality and positive feedback. *PLoS ONE*, 6:e18901.

Okubo, A. (1986). Dynamical aspects of animal grouping: Swarms, schools, flocks, and herds. *Advances in Biophysics*, 22:1–94.

Okubo, A. and Levin, S. A. (2001). *Diffusion and Ecological Problems: Modern Perspectives*. Springer-Verlag, Berlin, Germany.

Østergaard, E. H., Sukhatme, G. S., and Matarić, M. J. (2001). Emergent bucket brigading: a simple mechanisms for improving performance in multi-robot constrained-space foraging tasks. In *Proceedings of the fifth international conference on Autonomous agents (AGENTS'01)*, pages 29–35, New York, NY, USA. ACM.

Prorok, A., Correll, N., and Martinoli, A. (2011). Multi-level spatial models for swarm-robotic systems. *The International Journal of Robotics Research*, 30(5):574–589.

Saffre, F., Furey, R., Krafft, B., and Deneubourg, J.-L. (1999). Collective decision-making in social spiders: Dragline-mediated amplification process acts as a recruitment mechanism. *J. theor. Biol.*, 198:507–517.

Schmickl, T. and Hamann, H. (2011). BEECLUST: A swarm algorithm derived from honeybees. In Xiao, Y., editor, *Bio-inspired Computing and Communication Networks*. CRC Press.

Schneider-Fontán, M. and Matarić, M. J. (1996). A study of territoriality: The role of critical mass in adaptive task division. In *From animals to animats IV*, pages 553–561. MIT Press.

Seeley, T. D., Camazine, S., and Sneyd, J. (1991). Collective decision-making in honey bees: how colonies choose among nectar sources. *Behavioral Ecology and Sociobiology*, 28(4):277–290.

Strogatz, S. H. (2001). Exploring complex networks. *Nature*, 410(6825):268–276.

Vicsek, T. and Zafeiris, A. (2012). Collective motion. *Physics Reports*, 517(3-4):71–140.

Yates, C. A., Erban, R., Escudero, C., Couzin, I. D., Buhl, J., Kevrekidis, I. G., Maini, P. K., and Sumpter, D. J. T. (2009). Inherent noise can facilitate coherence in collective swarm motion. *Proceedings of the National Academy of Sciences*, 106(14):5464–5469.